AIAA JOURNAL
Vol. 44, No. 11, November 2006

Nonlinear Dynamic Sensitivities of Structures Using Combined Approximations

M. Bogomolni,* U. Kirsch,† and I. Sheinman‡
Technion—Israel Institute of Technology, 32000 Haifa, Israel

DOI: 10.2514/1.20769

Calculation of design sensitivities involves much computational effort, particularly for nonlinear dynamic response of large structures. Modal analysis is often not effective for such problems, because eigenproblems must be solved many times. Approximation concepts, which are used to reduce the computational cost involved in structural analysis, are usually not sufficiently accurate for sensitivity analysis. In this study, approximate reanalysis concepts are used to improve the efficiency of nonlinear dynamic sensitivity analysis. Efficient evaluation of the derivatives, using modal analysis, finite difference of eigenpairs, and the recently developed combined approximations approach, is presented. Several approximate solution procedures are developed and compared in terms of the efficiency and the accuracy of the results. It is shown that some of the approximations presented reduce significantly the computational effort and provide sufficiently accurate results.

I. Introduction

DESIGN sensitivity analysis of structures deals with the calculation of the response derivatives with respect to the design variables. These derivatives are used in the solution of various problems such as design optimization, generation of response approximations, including approximate reanalysis models, and explicit approximations of the constraint functions in terms of the structural parameters. Sensitivities are required also for assessing the effects of uncertainties in the structural properties on the system response.

Calculation of design sensitivities involves much computational effort, particularly for nonlinear dynamic response of large structures. As a result, there has been much interest in efficient procedures for calculating the sensitivity coefficients. Early and recent developments in methods for sensitivity analysis are discussed in various studies [1–4]. Methods of sensitivity analysis for discretized systems can be divided into the following classes:

1) Finite-difference methods are easy to implement but might involve numerous repeated analyses and high computational cost, particularly in large problems. The efficiency can be improved by using fast reanalysis techniques, but finite-difference approximations might have accuracy problems.

2) Analytical methods provide exact solutions but might not be easy to implement in some problems.

3) Semi-analytical methods are based on a compromise between finite-difference methods and analytical methods. These methods are easy to implement but might provide inaccurate results.

In general, the main factors considered in choosing a suitable sensitivity analysis method for a specific application include the accuracy, the computational effort, and the ease-of-implementation. The quality of the results and efficiency of the calculations are usually two conflicting factors. That is, higher accuracy is often achieved at the expense of more computational effort.

Dynamic sensitivity analysis has been demonstrated by several authors. In [5], the mode superposition approach has been considered for linear response. Assuming harmonic loading, the response sensitivities were evaluated by direct differentiation of the equations of motion. In several studies [4,6], the unconditionally stable implicit numerical equation was directly derived. Many authors [4,6–9] use the available factorized coefficient matrix in the sensitivity calculations. Some recent studies [4,7–10] are devoted to nonlinear dynamic sensitivities. A direct differentiation method [7,8], global finite differences, and a semi-analytical method [9] were used.

Approximation concepts are often used to reduce the computational cost involved in repeated analysis of structures [11]. However, most approximations that are adequate for structural reanalysis are not sufficiently accurate for sensitivity analysis. Accuracy problems may arise, particularly, in cases of nonlinear dynamic response. In this study, approximation concepts are used to improve the efficiency of nonlinear dynamic sensitivity analysis. Given the results of exact analysis for an initial design, finite-difference derivatives are evaluated efficiently by the recently developed combined approximations (CA) approach [11,12]. Originally, the approach was developed for linear static problems. Recently, accurate results were reported also for eigenproblem reanalysis [13,14] and dynamic reanalysis [15,16]. Calculation of analytical derivatives using approximate analysis models have been demonstrated previously [17,18]. It was found that accurate results can be achieved, but such calculations might not be easy to implement.

It was demonstrated recently that accurate derivatives can be achieved efficiently by the CA approach for eigenproblems [19] and linear dynamic problems [20]. In this study, approximate reanalysis is used to improve the efficiency of nonlinear dynamic sensitivity analysis. The analysis problem is first presented. Several procedures for evaluating the response derivatives, using modal analysis, finite differences, and the combined approximations approach are then developed and compared in terms of the efficiency and the accuracy. It is shown that some of the procedures presented reduce significantly the computational effort and provide sufficiently accurate results.

II. Nonlinear Dynamic Analysis

A. Problem Formulation

Consider the equations of motion at time t for a system subjected to dynamic forces:

$$\mathbf{M}\,{}^{t}\ddot{\boldsymbol{r}} + \mathbf{C}\,{}^{t}\dot{\boldsymbol{r}} + {}^{t}\boldsymbol{F}_{s} = {}^{t}\boldsymbol{R} \tag{1}$$

where $\mathbf{M}$ is the mass matrix, $\mathbf{C}$ is the damping matrix, ${}^{t}\boldsymbol{r}$ is the displacement vector, ${}^{t}\dot{\boldsymbol{r}}$ is the velocity vector, ${}^{t}\ddot{\boldsymbol{r}}$ is the acceleration vector, ${}^{t}\boldsymbol{F}_{s}$ is the inelastic resisting force vector, and ${}^{t}\boldsymbol{R}$ is the external dynamic force vector. Writing the equations at time $t + \Delta t$

Received 28 October 2005; revision received 17 July 2006; accepted for publication 18 July 2006.

*Graduate Student, Department of Civil and Environmental Engineering.
†Professor, Department of Civil and Environmental Engineering.
‡Professor, Department of Civil and Environmental Engineering.

$$\mathbf{M}\,{}^{t+\Delta t}\ddot{\boldsymbol{r}} + \mathbf{C}\,{}^{t+\Delta t}\dot{\boldsymbol{r}} + {}^{t+\Delta t}\boldsymbol{F}_s = {}^{t+\Delta t}\boldsymbol{R} \tag{2}$$

and subtracting Eq. (1) from Eq. (2) we obtain the incremental equations:

$$\mathbf{M}\,{}^{t}\Delta\ddot{\boldsymbol{r}} + \mathbf{C}\,{}^{t}\Delta\dot{\boldsymbol{r}} + {}^{t}\Delta\boldsymbol{F}_s = {}^{t}\Delta\boldsymbol{R} \tag{3}$$

where

$$\begin{gathered} {}^{t}\boldsymbol{\Delta r} = {}^{t+\Delta t}\boldsymbol{r} - {}^{t}\boldsymbol{r} \qquad {}^{t}\Delta\dot{\boldsymbol{r}} = {}^{t+\Delta t}\dot{\boldsymbol{r}} - {}^{t}\dot{\boldsymbol{r}} \qquad {}^{t}\Delta\ddot{\boldsymbol{r}} = {}^{t+\Delta t}\ddot{\boldsymbol{r}} - {}^{t}\ddot{\boldsymbol{r}} \\ {}^{t}\boldsymbol{\Delta F}_s = {}^{t+\Delta t}\boldsymbol{F}_s - {}^{t}\boldsymbol{F}_s \qquad {}^{t}\Delta\boldsymbol{R} = {}^{t+\Delta t}\boldsymbol{R} - {}^{t}\boldsymbol{R} \end{gathered} \tag{4}$$

Using the first-order Taylor series approximations of the resisting force, we obtain

$${}^{t}\boldsymbol{\Delta F}_s = {}^{t+\Delta t}\boldsymbol{F}_s - {}^{t}\boldsymbol{F}_s \cong \frac{\partial {}^{t}\boldsymbol{F}_s}{\partial \boldsymbol{r}}\,{}^{t}\boldsymbol{\Delta r} \tag{5}$$

The tangent stiffness matrix at time t, ${}^{t}\mathbf{K}$, is given by

$${}^{t}\mathbf{K} = \frac{\partial {}^{t}\boldsymbol{F}_s}{\partial \boldsymbol{r}} \tag{6}$$

Thus, Eq. (5) can be expressed as

$${}^{t}\boldsymbol{\Delta F}_s \cong {}^{t}\mathbf{K}\,{}^{t}\boldsymbol{\Delta r} \tag{7}$$

Substituting Eq. (7) into Eq. (3) yields

$$\mathbf{M}\,{}^{t}\Delta\ddot{\boldsymbol{r}} + \mathbf{C}^{\mathrm{t}}\Delta\dot{\boldsymbol{r}} + {}^{t}\mathbf{K}\,{}^{t}\boldsymbol{\Delta r} = {}^{t}\Delta\boldsymbol{R} \tag{8}$$

Assuming that ${}^{t}\boldsymbol{r}$, ${}^{t}\dot{\boldsymbol{r}}$, and ${}^{t}\ddot{\boldsymbol{r}}$ are known and solving Eq. (8) by implicit numerical scheme for ${}^{t}\Delta\boldsymbol{r}$, ${}^{t}\Delta\dot{\boldsymbol{r}}$, and ${}^{t}\Delta\ddot{\boldsymbol{r}}$, we find

$${}^{t+\Delta t}\boldsymbol{r} = {}^{t}\boldsymbol{r} + {}^{t}\boldsymbol{\Delta r} \qquad {}^{t+\Delta t}\dot{\boldsymbol{r}} = {}^{t}\dot{\boldsymbol{r}} + {}^{t}\Delta\dot{\boldsymbol{r}} \qquad {}^{t+\Delta t}\ddot{\boldsymbol{r}} = {}^{t}\ddot{\boldsymbol{r}} + {}^{t}\Delta\ddot{\boldsymbol{r}} \tag{9}$$

The common procedures for dynamic analysis can be divided into two methods of solution: 1) direct integration, where Eqs. (8) are integrated using a numerical step-by-step procedure and 2) mode superposition, where the equilibrium equations are transformed into a form in which the step-by-step solution is less costly. In linear dynamic analysis, the mode superposition approach can be more effective than direct integration in cases where only the lowest mode shapes may be considered and the integration must be carried out for many time steps. In nonlinear dynamic analysis, the structure properties, the mode shapes, and the frequencies change during the solution process. Thus, a major difficulty in using mode superposition is the need to repeat the eigenproblem solutions due to these changes. To overcome this difficulty, various approximations are proposed in this study.

B. Analysis by Mode Superposition

We use the following transformations from the nodal displacements ${}^{t}\Delta\boldsymbol{r}$ to the generalized displacements ${}^{t}\Delta\mathbf{Z}$:

$$\begin{gathered} {}^{t}\Delta\boldsymbol{r} = \sum_{k=1}^{p} {}^{t}\boldsymbol{\Phi}_k\,{}^{t}\Delta Z_k = {}^{t}\boldsymbol{\Phi}\,{}^{t}\Delta\mathbf{Z} \qquad {}^{t}\Delta\dot{\boldsymbol{r}} = {}^{t}\boldsymbol{\Phi}\,{}^{t}\Delta\dot{\mathbf{Z}} \\ {}^{t}\Delta\ddot{\boldsymbol{r}} = {}^{t}\boldsymbol{\Phi}\,{}^{t}\Delta\ddot{\mathbf{Z}} \end{gathered} \tag{10}$$

where ${}^{t}\boldsymbol{\Phi}_k$ are the eigenvectors at time t, p is the number of mode shapes considered ($p \ll n$, n being the number of degrees of freedom), and ${}^{t}\boldsymbol{\Phi}$ is the matrix of eigenvectors.

The eigenvectors ${}^{t}\boldsymbol{\Phi}_k$ and eigenvalues ${}^{t}\lambda_k$ are obtained by solving the eigenproblem:

$${}^{t}\mathbf{K}\,{}^{t}\boldsymbol{\Phi}_k = {}^{t}\lambda_k \mathbf{M}\,{}^{t}\boldsymbol{\Phi}_k \qquad k = 1, 2, \ldots, p \tag{11}$$

Assuming proportional damping, substituting Eqs. (10) into Eq. (8), and premultiplying the resulting equations by ${}^{t}\boldsymbol{\Phi}_k$, we obtain the p uncoupled equations:

$$\mathbf{I}\,{}^{t}\Delta\ddot{\mathbf{Z}} + {}^{t}\mathbf{C}_d\,{}^{t}\Delta\dot{\mathbf{Z}} + {}^{t}\boldsymbol{\Omega}^{2\,t}\Delta\mathbf{Z} = {}^{t}\mathbf{P} \tag{12}$$

where

$${}^{t}\mathbf{C}_d = {}^{t}\boldsymbol{\Phi}^T\mathbf{C}\,{}^{t}\boldsymbol{\Phi} \qquad {}^{t}\boldsymbol{\Omega}^2 = {}^{t}\boldsymbol{\Phi}^{T\,t}\mathbf{K}\,{}^{t}\boldsymbol{\Phi} \qquad {}^{t}\mathbf{P} = {}^{t}\boldsymbol{\Phi}^{T\,t}\Delta\mathbf{R} \tag{13}$$

In these equations, the mass matrix in normalized coordinates $\mathbf{I} = {}^{t}\boldsymbol{\Phi}^T\mathbf{M}\,{}^{t}\boldsymbol{\Phi}$ is an identity matrix. The damping matrix ${}^{t}\mathbf{C}_d$ and the stiffness matrix ${}^{t}\boldsymbol{\Omega}^2$ in these coordinates are diagonal low-order matrices. The diagonal elements of these matrices are $2\xi_k\,{}^{t}\omega_k$ and ${}^{t}\omega_k^2 = {}^{t}\lambda_k$, respectively, where ξ_k are the damping ratios and ${}^{t}\omega_k$ are the free vibration frequencies. Thus, the p individual equations of motion are

$${}^{t}\Delta\ddot{Z}_k + 2\xi_k\,{}^{t}\omega_k\,{}^{t}\Delta\dot{Z}_k + {}^{t}\omega_k^{2\,t}\Delta Z_k = {}^{t}P_k \qquad k = 1, \ldots, p \tag{14}$$

In this study, we solve Eq. (14) by the Newmark method. During the solution process, we have to calculate ${}^{t}Z_k$, ${}^{t}\dot{Z}_k$, and ${}^{t}\ddot{Z}_k$. For this purpose, we use transformations from ${}^{t}\boldsymbol{r}$ to ${}^{t}\mathbf{Z}$, similar to Eqs. (10), premultiply both sides by ${}^{t}\boldsymbol{\Phi}_k^T\mathbf{M}$ and rearrange to obtain

$${}^{t}Z_k = \frac{{}^{t}\boldsymbol{\Phi}_k^T\mathbf{M}\,{}^{t}\boldsymbol{r}}{{}^{t}\boldsymbol{\Phi}_k^T\mathbf{M}\,{}^{t}\boldsymbol{\Phi}_k} \qquad {}^{t}\dot{Z}_k = \frac{{}^{t}\boldsymbol{\Phi}_k^T\mathbf{M}\,{}^{t}\dot{\boldsymbol{r}}}{{}^{t}\boldsymbol{\Phi}_k^T\mathbf{M}\,{}^{t}\boldsymbol{\Phi}_k} \qquad {}^{t}\ddot{Z}_k = \frac{{}^{t}\boldsymbol{\Phi}_k^T\mathbf{M}\,{}^{t}\ddot{\boldsymbol{r}}}{{}^{t}\boldsymbol{\Phi}_k^T\mathbf{M}\,{}^{t}\boldsymbol{\Phi}_k} \tag{15}$$

Determining the displacements, velocities, and accelerations, the element forces are checked for material nonlinearity. If any element is in the nonlinear region, we reduce the time steps to find the transition point of the material properties. If the force in any element has reached the elastic limit point, we use a smaller time step. A similar procedure is used for the unloading region. The main difficulty of this approach is that we have to repeat the eigenproblem solution many times in the nonlinear region.

In summary, the following steps are being repeated for each time interval Δt.

1) Assemble the updated stiffness matrix ${}^{t}\mathbf{K}$.

2) Solve the updated eigenproblem [Eq. (11)] and find the p requested eigenpairs ${}^{t}\lambda_k$ and ${}^{t}\boldsymbol{\Phi}_k$. Efficient solution of this step by the CA method will be presented in Sec. IV.B.

3) Find ${}^{t}\mathbf{C}_d$, ${}^{t}\boldsymbol{\Omega}^2$, and ${}^{t}\mathbf{P}$ [Eqs. (13)].

4) Evaluate ${}^{t}\Delta\mathbf{Z}$, ${}^{t}\Delta\dot{\mathbf{Z}}$, and ${}^{t}\Delta\ddot{\mathbf{Z}}$ by solving the p uncoupled equations [Eq. (12)].

5) Find ${}^{t}\Delta\boldsymbol{r}$, ${}^{t}\Delta\dot{\boldsymbol{r}}$, and ${}^{t}\Delta\ddot{\boldsymbol{r}}$ by Eqs. (10).

6) Evaluate ${}^{t+\Delta t}\boldsymbol{r}$, ${}^{t+\Delta t}\dot{\boldsymbol{r}}$, and ${}^{t+\Delta t}\ddot{\boldsymbol{r}}$ by Eq. (9).

7) Evaluate the member forces. If the stiffness coefficients do not change, go to step 4 for the next time step. Otherwise, reduce the time step size and go to step 1.

III. Analytical Derivatives

A. Solution by Direct Integration

For purposes of comparison, we consider also the direct integration approach. Differentiation of Eq. (8) with respect to X_j gives

$$\begin{aligned} \mathbf{M}\frac{\partial {}^{t}\Delta\ddot{\boldsymbol{r}}}{\partial X_j} + \mathbf{C}\frac{\partial {}^{t}\Delta\dot{\boldsymbol{r}}}{\partial X_j} + {}^{t}\mathbf{K}\frac{\partial {}^{t}\boldsymbol{\Delta r}}{\partial X_j} &= \frac{\partial {}^{t}\Delta\boldsymbol{R}}{\partial X_j} - \frac{\partial \mathbf{M}}{\partial X_j}\,{}^{t}\Delta\ddot{\boldsymbol{r}} - \frac{\partial \mathbf{C}}{\partial X_j}\,{}^{t}\Delta\dot{\boldsymbol{r}} \\ &\quad - \frac{\partial {}^{t}\mathbf{K}}{\partial X_j}\,{}^{t}\boldsymbol{\Delta r} \end{aligned} \tag{16}$$

Because Eqs. (8) and (16) have similar left-hand sides (identical coefficient matrices), we can solve efficiently the latter equation. Solving Eq. (16), we then find by differentiation of Eq. (9)

$$\frac{\partial {}^{t+\Delta t}\boldsymbol{r}}{\partial X_j} = \frac{\partial {}^{t}\boldsymbol{r}}{\partial X_j} + \frac{\partial {}^{t}\boldsymbol{\Delta r}}{\partial X_j} \tag{17}$$

$$\frac{\partial {}^{t+\Delta t}\dot{\boldsymbol{r}}}{\partial X_j} = \frac{\partial {}^{t}\dot{\boldsymbol{r}}}{\partial X_j} + \frac{\partial {}^{t}\boldsymbol{\Delta}\dot{\boldsymbol{r}}}{\partial X_j} \tag{18}$$

$$\frac{\partial^{t+\Delta t}\ddot{\boldsymbol{r}}}{\partial X_j} = \frac{\partial^t \ddot{\boldsymbol{r}}}{\partial X_j} + \frac{\partial^t \boldsymbol{\Delta}\ddot{\boldsymbol{r}}}{\partial X_j} \tag{19}$$

B. Solution by Mode Superposition

Differentiating Eqs. (10) with respect to X_j, we obtain

$$\frac{\partial^t \Delta \boldsymbol{r}}{\partial X_j} = \sum_{k=1}^{p}\left(\frac{\partial^t \boldsymbol{\Phi}_k}{\partial X_j}\Delta Z_k + {}^t\boldsymbol{\Phi}_k \frac{\partial \Delta Z_k}{\partial X_j}\right) \tag{20}$$

$$\frac{\partial^t \Delta \dot{\boldsymbol{r}}}{\partial X_j} = \sum_{k=1}^{p}\left(\frac{\partial^t \boldsymbol{\Phi}_k}{\partial X_j}\Delta \dot{Z}_k + {}^t\boldsymbol{\Phi}_k \frac{\partial \Delta \dot{Z}_k}{\partial X_j}\right) \tag{21}$$

$$\frac{\partial^t \Delta \ddot{\boldsymbol{r}}}{\partial X_j} = \sum_{k=1}^{p}\left(\frac{\partial^t \boldsymbol{\Phi}_k}{\partial X_j}\Delta \ddot{Z}_k + {}^t\boldsymbol{\Phi}_k \frac{\partial \Delta \ddot{Z}_k}{\partial X_j}\right) \tag{22}$$

The values of ${}^t\boldsymbol{\Phi}_k$, ${}^t\Delta Z$, ${}^t\Delta \dot{Z}$, and ${}^t\Delta \ddot{Z}$ are known from the solution of Eqs. (11) and (14).

To calculate the term $\partial^t \boldsymbol{\Phi}_k / \partial X_j$, we consider Eq. (11) and the conditions

$${}^t\boldsymbol{\Phi}_k{}^T \mathbf{M}\, {}^t\boldsymbol{\Phi}_k = 1 \tag{23}$$

Differentiating Eqs. (11) and (23) with respect to X_j and rearranging gives

$$\begin{aligned}({}^t\mathbf{K} - {}^t\lambda \mathbf{M})\frac{\partial^t \boldsymbol{\Phi}_k}{\partial X_j} - \frac{\partial^t \lambda_k}{\partial X_j}\mathbf{M}\, {}^t\boldsymbol{\Phi}_k &= -\left(\frac{\partial^t \mathbf{K}}{\partial X_j} - {}^t\lambda_k \frac{\partial \mathbf{M}}{\partial X_j}\right){}^t\boldsymbol{\Phi}_k \\ {}^t\boldsymbol{\Phi}_k^T \mathbf{M}\frac{\partial^t \boldsymbol{\Phi}_k}{\partial X_j} &= -\frac{1}{2}\, {}^t\boldsymbol{\Phi}_k^T \frac{\partial \mathbf{M}}{\partial X_j}\, {}^t\boldsymbol{\Phi}_k\end{aligned} \tag{24}$$

or, in matrix form

$$\begin{bmatrix} {}^t\mathbf{K} - {}^t\lambda_k \mathbf{M} & -\mathbf{M}\, {}^t\boldsymbol{\Phi}_k \\ {}^t\boldsymbol{\Phi}_k^T \mathbf{M} & 0 \end{bmatrix}\begin{Bmatrix} \frac{\partial^t \boldsymbol{\Phi}_k}{\partial X_j} \\ \frac{\partial^t \lambda_k}{\partial X_j} \end{Bmatrix} = -\begin{Bmatrix} \left(\frac{\partial^t \mathbf{K}}{\partial X_j} - \lambda \frac{\partial \mathbf{M}}{\partial X_j}\right){}^t\boldsymbol{\Phi}_k \\ \frac{1}{2}\boldsymbol{\Phi}_k^T \frac{\partial \mathbf{M}}{\partial X_j}\, {}^t\boldsymbol{\Phi}_k \end{Bmatrix} \tag{25}$$

Several methods have been proposed to solve Eq. (25). In general, the solution involves much computational effort, because a matrix of the order $(n+1)$, n being the number of degrees of freedom, must be factorized many times, and forward and backward substitutions must be carried out for each design variable. In addition, the matrices $\partial^t \mathbf{K}/\partial X_j$ and $\partial \mathbf{M}/\partial X_j$ must be calculated.

If we are interested only in the derivatives of the eigenvalues, we premultiply the first of Eqs. (24) by ${}^t\boldsymbol{\Phi}_k^T$ and rearrange to obtain

$$\begin{aligned}\frac{\partial^t \lambda_k}{\partial X_j}\, {}^t\boldsymbol{\Phi}_k^T \mathbf{M}\, {}^t\boldsymbol{\Phi}_k = {}^t\boldsymbol{\Phi}_k^T\left(\frac{\partial^t \mathbf{K}}{\partial X_j} - \lambda_0 \frac{\partial \mathbf{M}}{\partial X_j}\right){}^t\boldsymbol{\Phi}_k + {}^t\boldsymbol{\Phi}_k^T({}^t\mathbf{K} \\ - {}^t\lambda_k \mathbf{M})\frac{\partial^t \boldsymbol{\Phi}_k}{\partial X_j}\end{aligned} \tag{26}$$

The eigenproblem ${}^t\boldsymbol{\Phi}_k^T\, {}^t\mathbf{K} = {}^t\lambda_k\, {}^t\boldsymbol{\Phi}_k^T \mathbf{M}$ can be written as ${}^t\boldsymbol{\Phi}_k^T({}^t\mathbf{K} - {}^t\lambda_k \mathbf{M}) = \mathbf{0}$, that is, the last term in Eq. (26) equals zero. Rearranging the resulting equation we obtain

$$\frac{\partial^t \lambda_k}{\partial X_j} = \frac{{}^t\boldsymbol{\Phi}_k^T\left(\frac{\partial^t \mathbf{K}}{\partial X_j} - {}^t\lambda_k \frac{\partial \mathbf{M}}{\partial X_j}\right){}^t\boldsymbol{\Phi}_k}{{}^t\boldsymbol{\Phi}_k^T \mathbf{M}\boldsymbol{\Phi}_k} \tag{27}$$

Note that this is only correct if the eigenvalue ${}^t\lambda_k$ is distinct. Several methods have been proposed to calculate the derivatives of the eigenvectors [4].

Returning to Eqs. (20–22), the terms $\partial^t \Delta Z_k/\partial X_j$, $\partial^t \Delta \dot{Z}_k/\partial X_j$, and $\partial^t \Delta \ddot{Z}_k/\partial X_j$ are computed by differentiation of Eq. (14) with respect to X_j:

$$\begin{aligned}\frac{\partial \Delta^t \ddot{Z}_k}{\partial X_j} + 2\, {}^t\omega_k \xi_k \frac{\partial \Delta^t \dot{Z}_k}{\partial X_j} + {}^t\omega_k^2 \frac{\partial^t \Delta Z_k}{\partial X_j} = \frac{\partial^t P_k}{\partial X_j} - 2\frac{\partial^t \omega_k}{\partial X_j}\xi_k \Delta^t \dot{Z}_k \\ - \frac{\partial^t \omega_k^2}{\partial X_j}\Delta^t Z_k\end{aligned} \tag{28}$$

Equation (28) is solved by Newmark's method. For this purpose, we have to evaluate $\partial^t Z_k/\partial X_j$, $\partial^t \dot{Z}_k/\partial X_j$, and $\partial^t \ddot{Z}_k/\partial X_j$. Consider the transformation

$${}^t\boldsymbol{r} = \sum_{k=1}^{p} {}^t\boldsymbol{\Phi}_k\, {}^tZ_k \tag{29}$$

Differentiating Eq. (29), we obtain

$$\frac{\partial^t \boldsymbol{r}}{\partial X_j} = \sum_{k=1}^{p}\left(\frac{\partial^t \boldsymbol{\Phi}_k}{\partial X_j}Z_k + {}^t\boldsymbol{\Phi}_k \frac{\partial Z_k}{\partial X_j}\right) \tag{30}$$

Premultiplying Eq. (30) by ${}^t\boldsymbol{\Phi}_k^T \mathbf{M}$, noting the orthogonality property ${}^t\boldsymbol{\Phi}^T \mathbf{M}\, {}^t\boldsymbol{\Phi} = \mathbf{I}$, and rearranging gives

$$\frac{\partial^t Z_k}{\partial X_j} = \frac{{}^t\boldsymbol{\Phi}_k^T \mathbf{M}[(\partial^t \boldsymbol{r}/\partial X_j) - \sum_{k=1}^{p}(\partial^t \boldsymbol{\Phi}_k/\partial X_j)^t Z_k]}{{}^t\boldsymbol{\Phi}_k^T \mathbf{M}\, {}^t\boldsymbol{\Phi}_k} \tag{31}$$

Similarly, we obtain for $\partial^t \dot{Z}_k/\partial X_j$ and $\partial^t \ddot{Z}_k/\partial X_j$

$$\frac{\partial^t \dot{Z}_k}{\partial X_j} = \frac{{}^t\boldsymbol{\Phi}_k^T \mathbf{M}[(\partial^t \dot{\boldsymbol{r}}/\partial X_j) - \sum_{k=1}^{p}(\partial^t \boldsymbol{\Phi}_k/\partial X_j)^t \dot{Z}_k]}{{}^t\boldsymbol{\Phi}_k^T \mathbf{M}\, {}^t\boldsymbol{\Phi}_k} \tag{32}$$

$$\frac{\partial^t \ddot{Z}_k}{\partial X_j} = \frac{{}^t\boldsymbol{\Phi}_k^T \mathbf{M}[(\partial^t \ddot{\boldsymbol{r}}/\partial X_j) - \sum_{k=1}^{p}(\partial^t \boldsymbol{\Phi}_k/\partial X_j)^t \ddot{Z}_k]}{{}^t\boldsymbol{\Phi}_k^T \mathbf{M}\, {}^t\boldsymbol{\Phi}_k} \tag{33}$$

In summary, starting with the initial conditions $\partial^0 \boldsymbol{r}/\partial X_j = \partial^0 \dot{\boldsymbol{r}}/\partial X_j = \mathbf{0}$, nonlinear dynamic sensitivity analysis involves the following calculations for each time step.

1) Compute the eigenpair derivatives $\partial^t \boldsymbol{\Phi}_k/\partial X_j$ and $\partial^t \lambda_k/\partial X_j$ $(k = 1, \ldots, p)$ by Eq. (25).

2) Compute $\partial^t Z_k/\partial X_j$, $\partial^t \dot{Z}_k/\partial X_j$, and $\partial^t \ddot{Z}_k/\partial X_j$ by Eqs. (31–33).

3) Compute the derivatives $\partial^t \Delta \mathbf{Z}/\partial X_j$, $\partial^t \Delta \dot{\mathbf{Z}}/\partial X_j$, and $\partial^t \Delta \ddot{\mathbf{Z}}/\partial X_j$ by solving Eqs. (28).

4) Compute $\partial^t \Delta \boldsymbol{r}/\partial X_j$, $\partial^t \Delta \dot{\boldsymbol{r}}/\partial X_j$, and $\partial^t \Delta \ddot{\boldsymbol{r}}/\partial X_j$ by Eqs. (20–22).

5) Compute $\partial^{t+\Delta t}\boldsymbol{r}/\partial X_j$, $\partial^{t+\Delta t}\dot{\boldsymbol{r}}/\partial X_j$, and $\partial^{t+\Delta t}\ddot{\boldsymbol{r}}/\partial X_j$ by Eqs. (17–19).

IV. Efficient Eigenpair Derivatives

A. Finite-Difference Derivatives

In this section, the problem of evaluating the eigenpair derivatives $\partial^t \boldsymbol{\Phi}_k/\partial X_j$ and $\partial^t \lambda_k/\partial X_j$ $(k = 1, \ldots, p)$ by finite differences is formulated. In the forward-difference method, the derivatives are approximated from the exact displacements at the original point X_0 and at the perturbed point $X_0 + \delta X$:

$$\frac{\partial^t \boldsymbol{\Phi}_k}{\partial X_j} = \frac{{}^t\boldsymbol{\Phi}_k(X_0 + \delta X) - {}^t\boldsymbol{\Phi}_k(X_0)}{\delta X} \tag{34}$$

where δX is the step size. The accuracy can be improved by adopting the central-difference approximation, where the derivatives are computed from the exact displacements at the two points $X_0 - \delta X$ and $X_0 + \delta X$ by

$$\frac{\partial^t \boldsymbol{\Phi}_k}{\partial X_j} = \frac{{}^t\boldsymbol{\Phi}_k(X_0 + \delta X) - {}^t\boldsymbol{\Phi}_k(X_0 - \delta X)}{2\delta X} \tag{35}$$

Finite-difference methods are the easiest to implement and therefore they are attractive in many applications. When ${}^t\mathbf{\Phi}_k(X_0)$ is known, application of Eq. (34) involves only one additional calculation of the displacements at $X_0 + \delta X$, whereas Eq. (35) requires calculation at the two points $X_0 - \delta X$ and $X_0 + \delta X$. For a problem with m design variables, finite difference derivative calculations require repetition of the analysis for $m + 1$ [Eq. (34)] or $2m + 1$ [Eq. (35)] different design points. This procedure is usually not efficient compared with, for example, analytical and semi-analytical methods. The efficiency of finite-difference derivatives can be improved significantly by the CA approach described next. Finite-difference approximations might have accuracy problems due to truncation errors or condition errors. A small step size δX will reduce the truncation error, but may increase the condition error. Considerations for choosing the forward-difference step size are discussed elsewhere [21].

B. Eigenproblem Reanalysis by Combined Approximations

Eigenproblem reanalysis by the CA method has been discussed in detail in previous studies [13,14]. For completeness of presentation, the solution procedure is briefly described in this section. Given an initial design, we assume that the corresponding stiffness matrix ${}^0\mathbf{K}$ is given in the decomposed form:

$$ {}^0\mathbf{K} = {}^0\mathbf{U}^{T\,0}\mathbf{U} \tag{36} $$

where ${}^0\mathbf{U}$ is an upper triangular matrix. The initial eigenpair ${}^0\mathbf{\Phi}$ and ${}^0\lambda$ (for simplicity of presentation, the subscript k is deleted) is obtained by solving the initial eigenproblem:

$$ {}^0\mathbf{K}\,{}^0\mathbf{\Phi} = {}^0\lambda\mathbf{M}\,{}^0\mathbf{\Phi} \tag{37} $$

Assume a perturbation δX in the design and a corresponding change ${}^t\delta\mathbf{K}$ (considering nonlinear effects) in the stiffness matrix. The modified matrix is given by

$$ {}^t\mathbf{K} = {}^0\mathbf{K} + {}^t\delta\mathbf{K} \tag{38} $$

The object is to estimate efficiently and accurately the requested eigenpair ${}^t\mathbf{\Phi}$ and ${}^t\lambda$ without solving the complete set of modified equations [Eq. (11)]:

$$ ({}^0\mathbf{K} + {}^t\delta\mathbf{K})\,{}^t\mathbf{\Phi} = {}^t\lambda\mathbf{M}\,{}^t\mathbf{\Phi} \tag{39} $$

The solution process involves the following steps.

1) Calculate the modified matrices ${}^t\mathbf{K}$ [Eq. (38)] and $\mathbf{M}$.

2) Calculate the matrix of basis vectors $\mathbf{r}_B$:

$$ \mathbf{r}_B = [\boldsymbol{r}_1, \boldsymbol{r}_2, \ldots, \boldsymbol{r}_s] \tag{40} $$

where $\boldsymbol{r}_1, \boldsymbol{r}_2, \ldots, \boldsymbol{r}_s$ are the basis vectors and s is much smaller than the number of degrees of freedom. For any requested eigenpair, the basis vectors are first determined by the terms of the binomial series:

$$ \boldsymbol{r}_1 = {}^0\mathbf{K}^{-1}\mathbf{M}\,{}^0\mathbf{\Phi} \qquad \boldsymbol{r}_k = -\mathbf{B}\boldsymbol{r}_{k-1} \tag{41} $$

where matrix $\mathbf{B}$ is defined as

$$ \mathbf{B} = {}^0\mathbf{K}^{-1\,t}\delta\mathbf{K} \tag{42} $$

It can be observed that calculation of each basis vector by Eq. (41) involves only forward and backward substitutions, because ${}^0\mathbf{K}$ is given in a decomposed form. Various means have been used to improve the accuracy [15,16,20], including central-difference expression for ${}^t\delta\mathbf{K}$, shifts of eigenvalues, Gram–Schmidt orthogonalizations of the basis vectors, and the higher mode shapes.

3) Calculate the reduced matrices $\mathbf{K}_R$ and $\mathbf{M}_R$ by

$$ \mathbf{K}_R = \mathbf{r}_B^{T\,t}\mathbf{K}\mathbf{r}_B \qquad \mathbf{M}_R = \mathbf{r}_B^T\mathbf{M}\mathbf{r}_B \tag{43} $$

4) Solve the reduced $s \times s$ eigenproblem for the first eigenpair λ_1, $\mathbf{y}_1$

$$ \mathbf{K}_R\boldsymbol{y}_1 = \lambda_1\mathbf{M}_R\boldsymbol{y}_1 \tag{44} $$

where $\boldsymbol{y}_1$ is a vector of unknown coefficients

$$ \boldsymbol{y}_1^T = \{\mathrm{y}_1, \mathrm{y}_2, \ldots, \mathrm{y}_s\} \tag{45} $$

Various methods (e.g. inverse vector iteration) can be used for this purpose.

5) Evaluate the requested mode shape ${}^t\mathbf{\Phi}$ by

$$ {}^t\mathbf{\Phi} = \mathrm{y}_1\mathbf{r}_1 + \mathrm{y}_2\mathbf{r}_2 + \ldots + \mathrm{y}_s\mathbf{r}_s = \mathbf{r}_B\mathbf{y}_1 \tag{46} $$

The requested eigenvalue is already given from Eq. (44) $\lambda = \lambda_1$.

It was found that high accuracy is often achieved with a very small number of basis vectors. In such cases, the preceding solution procedure is most effective.

V. Efficient Solution Procedures

It has been noted that the mode superposition approach is usually not effective in nonlinear dynamic analysis problems, because the eigenvalue problem must be solved repeatedly for each change in the stiffness coefficients. In this section, several solution procedures using mode superposition and the CA approach are presented. The efficiency of these procedures is compared with that of direct integration. It is shown that some of the approximation concepts presented reduce significantly the computational effort. Accuracy considerations are discussed in Sec. VI and typical results for simple numerical examples are demonstrated in Sec. VII.

A. Solution Procedures

The following solution procedures are considered in this section.

1) Solution by direct integration (DI) as presented in Sec. III.A. Analytical derivatives are obtained by the solution of Eqs. (16–19). It has been noted that, because Eqs. (8) and (16) have the same coefficient matrices in the left-hand side, we can solve efficiently the latter equation.

2) Mode superposition using exact analysis [MS(EX)] as presented in Sec. II.B. Solution by mode superposition is presented in Sec. III.B. The derivatives of the eigenpairs $\partial^t\mathbf{\Phi}_k/\partial X_j$ and $\partial^t\lambda_k/\partial X_j$ are calculated by forward finite differences, using exact analysis for both the original and the perturbed eigenproblems:

$$ \frac{\partial^t\mathbf{\Phi}_k}{\partial X_j} = \frac{{}^t\mathbf{\Phi}_{kEx}(X_0 + \delta X) - {}^t\mathbf{\Phi}_{kEx}(X_0)}{\delta X} \tag{47} $$

$$ \frac{\partial^t\lambda_k}{\partial X_j} = \frac{{}^t\lambda_{kEx}(X_0 + \delta X) - {}^t\lambda_{kEx}(X_0)}{\delta X} \tag{48} $$

3) Mode superposition using CA [MS(CA)] as presented in Secs. II.B and IV.B. The eigenpair derivatives are calculated by forward finite differences, using CA analysis for both the original and the perturbed eigenproblems:

$$ \frac{\partial^t\mathbf{\Phi}_k}{\partial X_j} = \frac{{}^t\mathbf{\Phi}_{kCA}(X_0 + \delta X) - {}^t\mathbf{\Phi}_{kCA}(X_0)}{\delta X} \tag{49} $$

$$ \frac{\partial^t\lambda_k}{\partial X_j} = \frac{{}^t\lambda_{kCA}(X_0 + \delta X) - {}^t\lambda_{kCA}(X_0)}{\delta X} \tag{50} $$

4) Mode superposition using exact analysis for the original eigenproblem and CA analysis for the perturbed eigenproblem [MS (EX)+MS(CA)]:

$$ \frac{\partial^t\mathbf{\Phi}_k}{\partial X_j} = \frac{{}^t\mathbf{\Phi}_{kCA}(X_0 + \delta X) - {}^t\mathbf{\Phi}_{kEx}(X_0)}{\delta X} \tag{51} $$

$$\frac{\partial {}^t\lambda_k}{\partial X_j} = \frac{{}^t\lambda_{kCA}(X_0 + \delta X) - {}^t\lambda_{kEx}(X_0)}{\delta X} \tag{52}$$

5) Mode superposition using exact analysis and approximate eigenvector sensitivities [MS(EX)+APP] . The eigenpair derivatives are calculated using the exact eigenpair values ${}^t\mathbf{\Phi}$ and ${}^t\lambda$, and the initial eigenpair derivatives $\partial^0\mathbf{\Phi}/\partial X$ and $\partial^0\lambda/\partial X$ as follows. We first calculate $\partial^t\lambda/\partial X$ by the exact expression [see Eqs. (23) and (27)]:

$$\frac{\partial {}^t\lambda_k}{\partial X_j} = \frac{{}^t\mathbf{\Phi}_{kEx}^T[(\partial {}^t\mathbf{K}/\partial X_j) - {}^t\lambda_{kEx}(\partial \mathbf{M}/\partial \mathbf{X}_j)]^t\mathbf{\Phi}_{kEx}}{{}^t\mathbf{\Phi}_{Ex}^T\mathbf{M}^t\mathbf{\Phi}_{Ex}}$$
$$= \frac{{}^t\mathbf{\Phi}_{kEx}^T[(\partial {}^t\mathbf{K}/\partial X_j) - {}^t\lambda_{kEx}(\partial \mathbf{M}/\partial \mathbf{X}_j)]^t\mathbf{\Phi}_{kEx}}{{}^0\mathbf{\Phi}_{kEx}^T[(\partial {}^0\mathbf{K}/\partial X_j) - {}^0\lambda_{kEx}(\partial \mathbf{M}/\partial \mathbf{X}_j)]^0\mathbf{\Phi}_{kEx}}\left(\frac{\partial^0\lambda_k}{\partial X_j}\right) \tag{53}$$

Then the eigenvector derivatives $\partial^t\mathbf{\Phi}_k/\partial X_j$ are assumed to be constant, using the approximation

$$\partial^t\mathbf{\Phi}_k/\partial X_j \cong \partial^0\mathbf{\Phi}_k/\partial X_j \tag{54}$$

6) Mode superposition using CA analysis and approximations [MS(CA)+APP]. The eigenpair derivatives are calculated by

$$\frac{\partial {}^t\lambda_k}{\partial X_j} = \frac{{}^t\mathbf{\Phi}_{kCA}^T[(\partial {}^t\mathbf{K}/\partial X_j) - {}^t\lambda_{kCA}(\partial \mathbf{M}/\partial X_j)]^t\mathbf{\Phi}_{kCA}}{{}^0\mathbf{\Phi}_{kEx}^T[(\partial {}^0\mathbf{K}/\partial X_j) - {}^0\lambda_{kEx}(\partial \mathbf{M}/\partial X_j)]^0\mathbf{\Phi}_{kEx}}\left(\frac{\partial^0\lambda_k}{\partial X_j}\right) \tag{55}$$

$$\partial^t\mathbf{\Phi}_k/\partial X_j \cong \partial^0\mathbf{\Phi}_k/\partial X_j \tag{56}$$

B. Efficiency Evaluation

It has been noted that, in general, the accuracy of the results and efficiency of the calculations are two conflicting factors. That is, higher accuracy is often achieved at the expense of more computational effort. In this section, the efficiency of various solution procedures is compared.

Consider a system of n degrees of freedom (DOF). N is the number of time steps, p is the number of requested mode shapes (usually $p \ll n$), m is the number of design variables, m_k is the half bandwidth of the stiffness matrix, and s is the number of basis vectors considered in the CA method. The parameter α represents the fraction of time that the stiffness matrix is updated ($\alpha = 0.2$ means that during 20% of the loading time, the stiffness matrix is updated due to nonlinearity). The number of main algebraic operations [22], needed for analysis and sensitivity analysis by the various procedures considered in this study, is shown in Table 1. For illustrative purposes, assume

$$N = 5000 \quad p = 5 \quad m = 20, 100 \quad m_k = n^{0.5} \quad s = 3 \quad \alpha = 0.2$$

The total number of algebraic operations vs the number of DOF for the various solution procedures is shown in Fig. 1. Comparing solutions by DI and MS(EX), it is observed that the number of algebraic operations in the latter case is significantly larger. As expected, this number is reduced by the MS(EX)+MS(CA) and even more by the MS(CA) procedure. The best efficiency is obtained by the procedure MS(CA)+APP, where mode superposition, the CA method, and the approximations of Eqs. (55) and (56) are used. The relationship between the number of operations involved in DI and MS(CA)+APP, shown in Fig. 2, indicates that sensitivity analysis by the latter procedure reduces significantly the computational effort. Thus, it would be useful to study whether the results obtained by this procedure are sufficiently accurate.

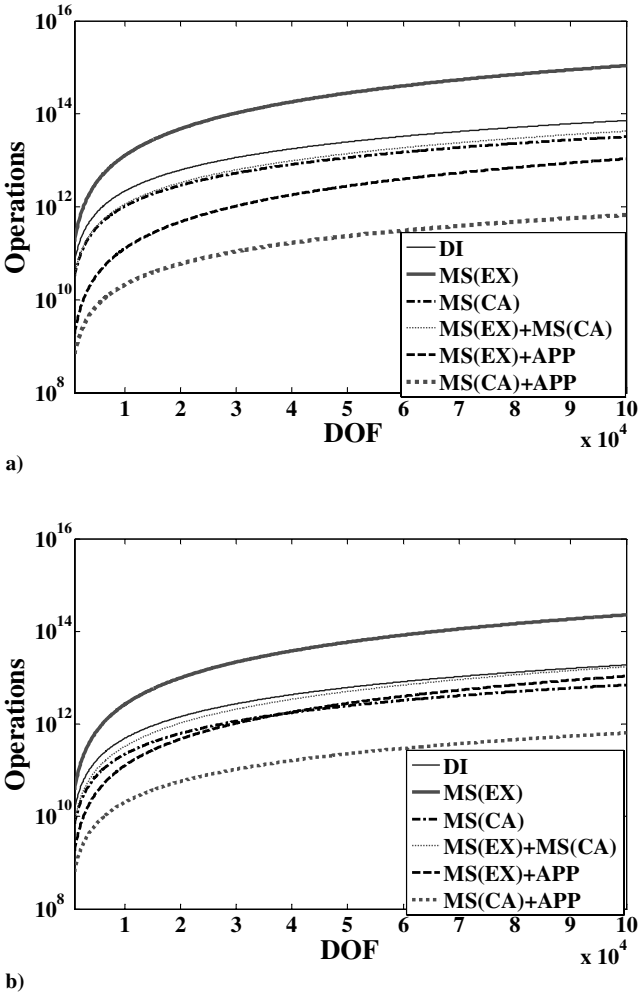

Fig. 1 Algebraic operations vs the number of DOF for various procedures: a) $m = 100$ and b) $m = 20$.

VI. Accuracy Considerations

As noted earlier, the mode superposition approach is usually not effective for nonlinear dynamic analysis and sensitivity analysis, because the eigenproblem must be solved repeatedly many times during the solution process. In recent studies, efficient procedures based on the CA approach for nonlinear dynamic reanalysis [16] and linear dynamic sensitivity analysis [20] have been presented. In this study, procedures for nonlinear dynamic sensitivity analysis are developed. The latter procedures are intended to reduce the computational effort and to provide results that are sufficiently accurate. Efficiency considerations of the procedures have been demonstrated in Sec. V and accuracy considerations are discussed in this section.

Table 1 Number of algebraic operations

Procedure	Analysis	Sensitivity Analysis
DI	$(3nm_k)N + (1+\alpha N)(\frac{1}{2}nm_k^2 + \frac{3}{2}nm_k)$	$(3nm_k)Nm + (1+\alpha N)3nm_km$
MS(EX)	$(3p)N + (nm_k^2 + 5pnm_k)(1+\alpha N)$	$(2p)N + (nm_k^2 + 5pnm_k)(1+\alpha N)m$
MS(CA)	$(3p)N + [2(nm_k)(s-1)p + ps^3](1+\alpha N)$	$(2p)N + [2(nm_k)(s-1)p + ps^3](1+\alpha N)m$
MS(EX)+MS(CA)	$(3p)N + (nm_k^2 + 5pnm_k)(1+\alpha N)$	$(2p)N + [2(nm_k)(s-1)p + ps^3](1+\alpha N)m$
MS(EX)+APP	$(3p)N + (nm_k^2 + 5pnm_k)(1+\alpha N)$	$(2p)N + [2(nm_k)sp + ps^3]m$
MS(CA)+APP	$(3p)N + [2(nm_k)(s-1)p + ps^3](1+\alpha N)$	$(2p)N + [2(nm_k)sp + ps^3]m$

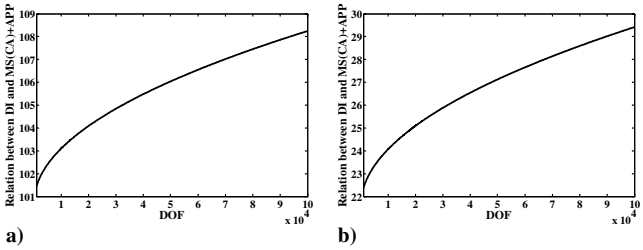

Fig. 2 The relationship between operations involved in DI and MS(CA) +APP: a) $m = 100$ and b) $m = 20$.

It has been noted that most approximations that are adequate for structural reanalysis are not sufficiently accurate for sensitivity analysis, particularly in cases of nonlinear dynamic response. In nonlinear dynamic analysis in general, and in nonlinear sensitivity analysis using order reduction in particular, accuracy problems may arise in various cases due to different reasons. Particularly challenging cases include structures undergoing large motions with significant geometric nonlinearity effects, as well as structures where local effects are important. The latter effects refer to behavior characteristics confined to localized areas of the structure, as well as the resulting stress information in areas of interest. Other challenging cases include shells or multiload-path statically indeterminate frames approaching buckling failure (local or global) with more complex boundary conditions and loads. To capture accurately the dynamic response of such nonlinear structures, it might be necessary to consider a relatively large number of mode shapes. In addition, when stresses are considered, convergence might be slower.

The accuracy of the results obtained by the CA approach has been investigated in previous studies [15,16,20,23,24]. Various procedures intended to improve the accuracy of the approximations have been developed, including Gram–Schmidt orthogonalizations of the approximate modes, shifts of the basis vectors, Gram–Schmidt orthogonalizations of the basis vectors, and reduction of truncation errors by central differences of the stiffness changes. It was found that by using these procedures, nearly exact solutions can be achieved. In addition, it has been proven that the CA method and the preconditioned conjugate gradient method, with an improved preconditioned matrix, provide identical results [23]. This result explains the improved convergence properties and provides available expressions for error evaluation [24]. In any case, the accuracy of the approximations can always be improved by considering additional basis vectors and the procedures mentioned previously.

Although the procedures presented might prove useful for different types of nonlinearity (e.g., material and geometrical nonlinearity), only simple numerical examples of material nonlinearity are demonstrated in the next section. The changes due to material nonlinearity might be local or global. It is recognized that the procedures developed in this study may provide inaccurate results for the more challenging cases mentioned earlier. For such cases, it might be necessary to develop additional means intended to improve the accuracy.

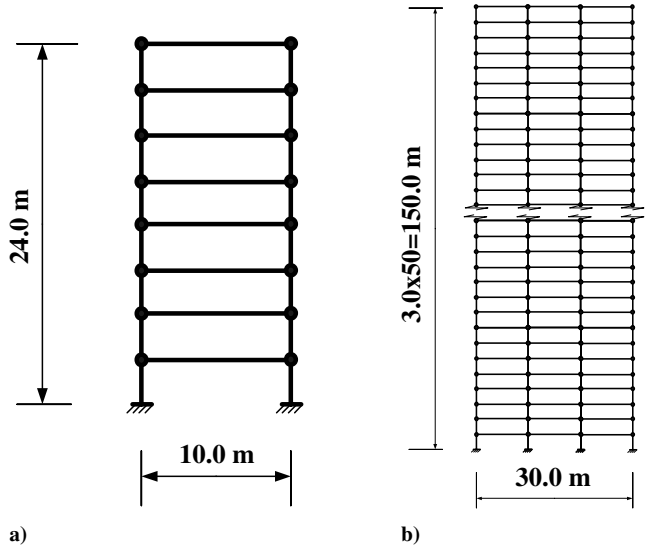

Fig. 3 Frame examples: a) eight-story frame and b) fifty-story frame.

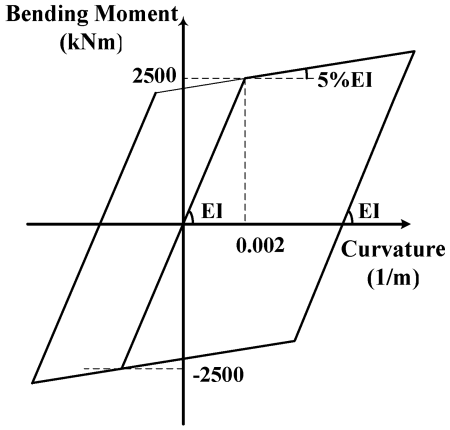

Fig. 4 Moment–curvature relation.

VII. Numerical Examples

In this section we consider the two frame examples of material nonlinearity shown in Fig. 3. The assumed moment–curvature relation is bilinear, as shown in Fig. 4, the modulus of elasticity is 3×10^7 kN/m^2, and the elastic limit stress is $\sigma_Y = 20000$ kN/m^2. The loading is the ground acceleration of the El Centro earthquake shown in Fig. 5, normalized to be at the 10% range of all earthquakes expected to appear in 50 years. Only horizontal inertia forces are considered.

A. Eight-Story Frame

Consider the eight-story frame shown in Fig. 3a. Damping is not considered and the time step is 0.025 s. The width of all elements is 0.5 m, the depth of all columns is 1.0 m, and the depth of all beams is 0.8 m. The total inertia force at each joint is due to the structure self-weight and an additional concentrated mass of 25 ton. It was found (by modal participation factors) that consideration of the first five mode shapes provides sufficiently accurate results. The CA analysis is used with only two basis vectors.

Derivatives of horizontal displacements at the top of the frame, with respect to the depth of the columns, using the MS(EX) procedure and finite-difference (FD) derivatives of displacements

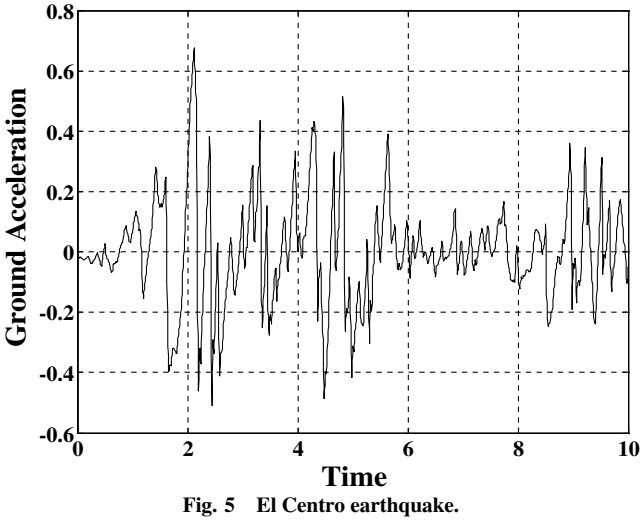

Fig. 5 El Centro earthquake.

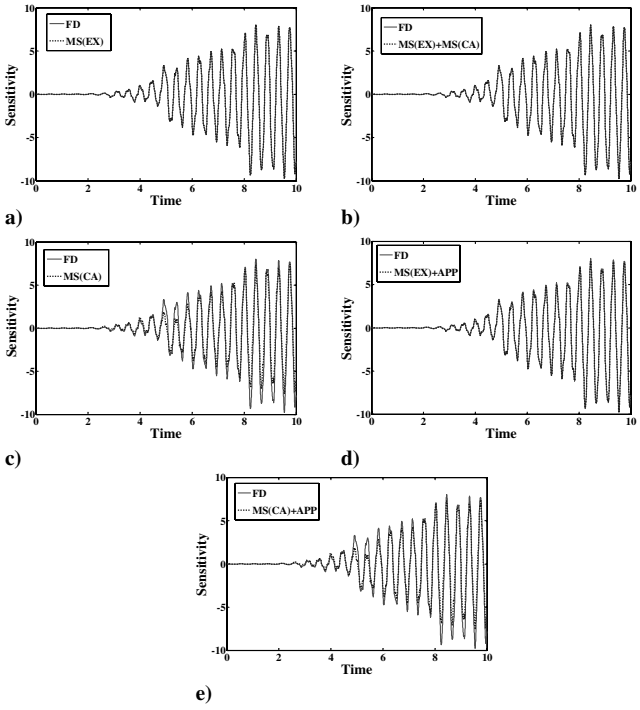

Fig. 6 Eight-story frame; displacement sensitivities obtained by: a) FD and MS(EX), b) FD and MS(EX)+MS(CA), c) FD and MS(CA), d) FD and MS(EX)+APP, and e) FD and MS(CA)+APP.

using exact analysis and a very small perturbation

$$\frac{\partial \mathbf{r}}{\partial X_j} = \frac{\mathbf{r}_{Ex}(X_0 + \delta X) - \mathbf{r}_{Ex}(X_0)}{\delta X} \tag{57}$$

are shown in Fig. 6a. It is observed that the results obtained by the two methods are practically the same. Thus, sensitivities calculated by the FD procedure will be used as a reference in comparing the results obtained by the procedures MS(EX)+MS(CA), MS(CA), MS(EX)+APP, and MS(CA)+APP, shown in Figs. 6b–6e. Figure 6b shows that high accuracy is achieved by the MS(EX)+MS(CA) procedure. Figure 6c shows that the results obtained by MS(CA) are less accurate then those obtained by the former MS(EX)+MS(CA) procedure. Figure 6d shows that high accuracy is achieved by the MS(EX)+APP procedure. Figure 6e shows that the results obtained by MS(CA)+APP are less accurate then those obtained by the former MS(EX)+APP procedure.

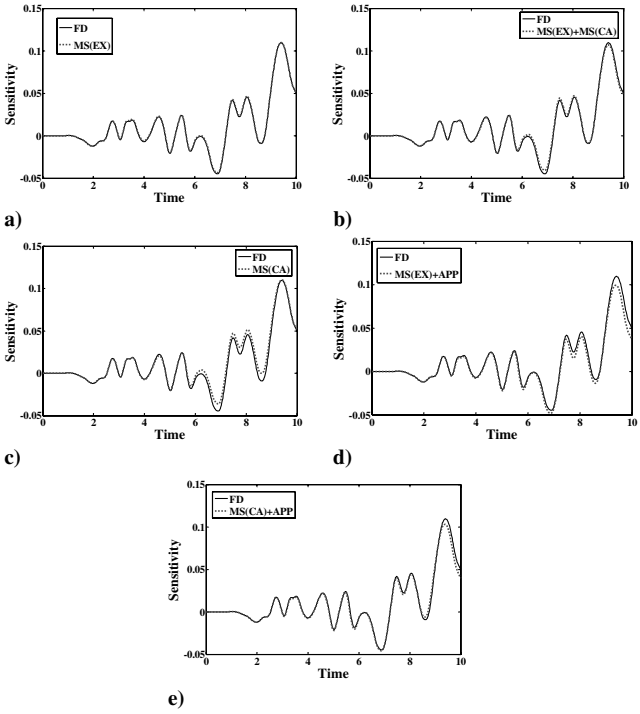

Fig. 7 Fifty-story frame; displacement sensitivities obtained by: a) FD and MS(EX), b) FD and MS(EX)+MS(CA), c) FD and MS(CA), d) FD and MS(EX)+APP, and e) FD and MS(CA)+APP.

B. Fifty-Story Frame

Consider the 50-story frame shown in Fig. 3b. The damping ratios for all modes are 0.05, the number of degrees of freedom is 600, and the time step is 0.02 s. The width and depth of all elements are 0.5 and 1.0 m, respectively. The inertia force is due to the frame self-weight and an additional concentrated mass of 50 ton in an internal joint and 25 ton in an external joint. It was found that the first eight mode shapes provide sufficiently accurate results. The CA analysis is used with nine basis vectors.

Derivatives of horizontal displacements at the top of the frame, with respect to the depth of the columns in the first floor, using the MS(EX) procedure and finite-difference derivatives of displacements using exact analysis are shown in Fig. 7a. It is observed that the results obtained by the two methods are practically the same. Thus, sensitivities calculated by the FD procedure will be used as a reference in comparing the results obtained by the procedures MS(EX)+MS(CA), MS(CA), MS(EX)+APP, and MS(CA)+APP, shown in Figs. 7b–7e. Figure 7b demonstrates that high accuracy is achieved by the MS(EX)+MS(CA) procedure. Figure 7c shows that the results obtained by MS(CA) are less accurate then those obtained by the former MS(EX)+MS(CA) procedure. Figures 7d and 7e show that good accuracy is achieved by both the MS(EX)+APP and the MS(CA)+APP procedures.

VIII. Conclusions

Calculation of repeated design sensitivities for nonlinear dynamic response of large structures involves much computational effort. Modal analysis is usually not effective for such problems, because eigenproblems must be solved repeatedly many times during the solution process. Approximation concepts, which are used to reduce the computational cost involved in structural reanalysis, are usually not sufficiently accurate for sensitivity analysis, particularly in cases of nonlinear dynamic response.

In this study, approximate reanalysis concepts are used to improve the efficiency of nonlinear dynamic sensitivity analysis. Efficient evaluation of the derivatives using modal analysis, finite difference of eigenpairs, and the recently developed CA approach is presented. Several approximate solution procedures are developed and compared in terms of the efficiency and the accuracy of the results. Some of the approximations presented reduce significantly the computational effort and provide sufficiently accurate results. As expected, higher accuracy is usually achieved for those procedures that involve more computational effort. However, the results obtained for typical numerical examples indicate that all procedures provide good approximations. Thus, the more efficient procedures can be used in many cases where the evaluated sensitivities are sufficiently accurate.

In previous developments of the CA approach, the problem complexity has been gradually increased. Initially, only linear static reanalysis and sensitivity analysis problems have been introduced. Later, reanalysis and sensitivity analysis for eigenproblems and linear dynamic problems have been presented. Recently, linear dynamic sensitivity analysis has been developed. In all the above cases, first the efficiency of the calculations was improved and the accuracy of the results was demonstrated for simple numerical examples. Then various means have been developed to improve the accuracy of the results for more challenging cases. These means include Gram–Schmidt orthogonalizations of the approximate modes, shifts of the basis vectors, Gram–Schmidt orthogonalizations of the basis vectors, and reduction of truncation errors by central differences of the stiffness changes. Using these means, nearly exact

solutions can be achieved. In any case, the errors involved in the approximations can be evaluated and the accuracy can always be improved by considering additional basis vectors.

Similarly, in this study, procedures for nonlinear dynamic sensitivity analysis have been developed, the efficiency of the calculations has been compared, and the accuracy of the results has been demonstrated for simple numerical examples. Although the procedures presented might be suitable for different types of nonlinearity (e.g., material or geometrical nonlinearity), only simple problems related to material nonlinearity have been considered for purposes of demonstration. It is recognized that for the more challenging cases of geometrical nonlinearity, the procedures developed in this study may provide inaccurate results. For such cases, it might be necessary to develop additional means intended to improve the accuracy.

References

[1] Haug, E. J., Choi, K. K., and Komkov, V., *Design Sensitivity Analysis of Structural System*, Academic Press, New York, 1986.

[2] Haftka, R. T., and Adelman, H. M., "Recent Developments in Structural Sensitivity Analysis," *Structural Optimization*, Vol. 1, No. 3, 1989, pp. 137–151.

[3] Haftka, R. T., and Gurdal, Z., *Elements of Structural Optimization*, 3rd ed., Kluwer, Dordrecht, The Netherlands, 1993.

[4] van Keulen, F., Haftka, R. T., and Kim, N. H., "Review of Options for Design Sensitivity Analysis. Part 1: Linear Systems," *Computer Methods in Applied Mechanics and Engineering*, Vol. 194, Nos. 30–33, 2005, pp. 3213–3243.

[5] Kramer, G. J., and Grierson, D. E., "Computer Automated Design of Structures Under Dynamic Loads," *Computers and Structures*, Vol. 32, No. 2, 1989, pp. 313–325.

[6] Kim, N. H., and Choi, K. K., "Design Sensitivity Analysis and Optimization of Nonlinear Transient Dynamics," AIAA Paper 2000-4905, 2000.

[7] Barbato, M., and Conte, J. P., "Finite Element Response Sensitivity Analysis: A Comparison Between Force-Based and Displacement-Based Frame Element Models," *Computer Methods in Applied Mechanics and Engineering*, Vol. 194, Nos. 12–16, 2005, pp. 1479–1512.

[8] Conte, J. P., Barbato, M., and Spacone, E., "Finite Element Response Sensitivity Analysis Using Force-Based Frame Models,". *International Journal for Numerical Methods in Engineering*, Vol. 59, No. 13, 2004, pp. 1781–1820.

[9] Okubo, S., and Tortorelli, D. A., "Control of Nonlinear, Continuous, Dynamic System Via Finite Elements, Sensitivity Analysis, and Optimization," *Structural and Multidisciplinary Optimization*, Vol. 26, Nos. 3–4, 2004, pp. 183–199.

[10] Falco, S. A., Afonso, S. M. B., and Vaz, L. E., "Analysis and Optimal Design of Plates and Shells Under Dynamic Loads—I: Finite Element and Sensitivity Analysis," *Structural and Multidisciplinary Optimization*, Vol. 27, No. 3, 2004, pp. 189–196.

[11] Kirsch, U., *Design-Oriented Analysis of Structures*, Kluwer, Dordrecht, The Netherlands, 2002.

[12] Kirsch, U., "A Unified Reanalysis Approach for Structural Analysis, Design and Optimization," *Structural and Multidisciplinary Optimization*, Vol. 25, No. 3, 2003, pp. 67–85.

[13] Kirsch, U., "Approximate Vibration Reanalysis of Structures," *AIAA Journal*, Vol. 41, No. 3, 2003, pp. 504–511.

[14] Kirsch, U., and Bogomolni, M., "Procedures for Approximate Eigenproblem Reanalysis of Structures," *International Journal for Numerical Methods in Engineering*, Vol. 60, 2004, pp. 1969–1986.

[15] Kirsch, U., Bogomolni, M., and Sheinman, I., "Efficient Dynamic Reanalysis of Structures," *Journal of Structural Engineering* (submitted for publication).

[16] Kirsch, U., Bogomolni, M., and Sheinman, I., "Nonlinear Dynamic Reanalysis by Combined Approximations," *Computer Methods in Applied Mechanics and Engineering*, Vol. 195, Nos. 33–36, 2006, pp. 4420–4432.

[17] Kirsch, U., "Effective Sensitivity Analysis for Structural Optimization," *Computer Methods in Applied Mechanics and Engineering*, Vol. 117, Nos. 1–2, 1994, pp. 143–156.

[18] Kirsch, U., and Papalambros, P. Y., "Accurate Displacement Derivatives for Structural Optimization Using Approximate Reanalysis," *Computer Methods in Applied Mechanics and Engineering*, Vol. 190, No. 31, 2001, pp. 3945–3956.

[19] Kirsch, U., Bogomolni, M., and van Keulen, F., "Efficient Finite-Difference Design-Sensitivities," *AIAA Journal*, Vol. 43, No. 2, 2005, pp. 399–405.

[20] Bogomolni, M., Kirsch, U., and Sheinman, I., "Efficient Design Sensitivities of Structures Subjected to Dynamic Loading," *International Journal for Solids and Structures* (to be published).

[21] Burton, R. R., "Computing Forward-Difference Derivatives in Engineering Optimization," *Engineering Optimization*, Vol. 20, No. 3, 1992, pp. 205–224.

[22] Bathe, K. J., *Finite Element Procedures*, Prentice–Hall, Upper Saddle River, NJ, 1996.

[23] Kirsch, U., Kocvara, M., and Zowe, J., "Accurate Reanalysis of Structures by a Preconditioned Conjugate Gradient Method," *International Journal for Numerical Methods in Engineering*, Vol. 55, No. 2, 2002, pp. 233–251.

[24] Kirsch, U., Bogomolni, M., "Error Evaluation in Approximate Reanalysis of Structures," *Structural and Multidisciplinary Optimization*, Vol. 28, Nos. 2–3, 2004, pp. 77–86.

E. Livne
Associate Editor